

Article

Formation and Microbial Composition of Biofilms in Drip Irrigation System under Three Reclaimed Water Conditions

Tianzhi Wang ^{1,2,3,†}, Xingda Dai ^{1,†}, Tianjiao Zhang ¹, Changchun Xin ¹, Zucheng Guo ^{2,3,4} and Jiehua Wang ^{1,*} 

¹ School of Environmental Science & Engineering, Tianjin University, Tianjin 300350, China; wtzhi1992@126.com (T.W.); dxd_1998@tju.edu.cn (X.D.); zhang.tianjiao@hotmail.com (T.Z.); hadesxin@163.com (C.X.)

² Department of Hydraulic Engineering, College of Water Resources and Civil Engineering, China Agricultural University, Beijing 100083, China; guozucheng@163.com

³ Earth Engineering Center and Department of Earth and Environmental Engineering, Columbia University, New York, NY 10027, USA

⁴ China Everbright International LTD, Hongkong 999077, China

* Correspondence: jiehuawang@tju.edu.cn

† These authors contributed equally to this work.

Abstract: As the second source of water for cities, reclaimed water (RW) has become an effective solution to the problem of water scarcity in modern agriculture. However, the formation of biofilm in an RW distribution system seriously affects the performance of the system and has become a technical challenge in RW utilization. In this study, we first showed that several water quality parameters, including five-day biochemical oxygen demand (BOD₅), total bacteria count (TB), total nitrogen (TN), and Cl⁻ were the main factors affecting biofilm accumulation in the drip irrigation system (DIS), with the correlation coefficient averaging above 0.85. Second, after 392 to 490 h of system operation, the total biomass and extracellular polymer (EPS) accumulation rate of biofilms increased to a maximum of 0.72 g/m²·h and 0.027g/m²·h, respectively, making this time point a critical point for controlling biofilm accumulation and clogging of the system. Third, we examined changes in biofilm microbial composition over time on Illumina's MiSeq platform. High throughput sequencing data showed that bacterial community structure and microbial network interaction and modularity changed significantly between 392 and 490 h, resulting in maximum microbial diversity and community richness at 490 h. Spearman correlation analyses between genera revealed that *Sphingomonas* and *Rhodococcus* promote biofilm formation due to their hydrophobicity, while *Bacillus*, *Mariniradius*, and *Arthronema* may inhibit biofilm formation due to their antagonistic effects on other genera. In conclusion, this work has clarified the accumulation process and compositional changes of biofilms in agriculture DIS under different RW conditions, which provides a basis for improving RW utilization efficiency and reducing system maintenance costs.

Keywords: reclaimed water; drip distribution systems; biofilms; bacterial community; Illumina sequencing



Citation: Wang, T.; Dai, X.; Zhang, T.; Xin, C.; Guo, Z.; Wang, J. Formation and Microbial Composition of Biofilms in Drip Irrigation System under Three Reclaimed Water Conditions. *Water* **2022**, *14*, 1216. <https://doi.org/10.3390/w14081216>

Academic Editors: Yingxin Zhao and Thomas Helmer Pedersen

Received: 10 March 2022

Accepted: 6 April 2022

Published: 10 April 2022

Publisher's Note: MDPI stays neutral with regard to jurisdictional claims in published maps and institutional affiliations.



Copyright: © 2022 by the authors. Licensee MDPI, Basel, Switzerland. This article is an open access article distributed under the terms and conditions of the Creative Commons Attribution (CC BY) license (<https://creativecommons.org/licenses/by/4.0/>).

1. Introduction

As the world's total water resources decrease year by year, the demand for water for irrigation, power generation, industry, and municipal use is rapidly increasing in the face of rapid population growth, urbanization, and industrialization [1,2]. With global freshwater shortages expected to reach 40 percent by 2030, according to UNESCO, water reuse has become an indispensable solution to growing water scarcity. In many countries, such as Spain and the United States, the recycled water use rate is over 70 percent [3–6].

Agriculture accounts for a large proportion of global water consumption, and the use of reclaimed water (RW) as water for agriculture can effectively alleviate water pressure. For example, Israel and the United States use more than 46 percent of their RW for agricultural irrigation [7,8]. At the same time, appropriate irrigation methods can further save water

resources, and the agricultural drip irrigation system (DIS) is one of the safest and most reliable methods for distributing RW, due to its accuracy and controllability. However, because the diameter of the outlet channel of DIS is usually only 0.5–1.2 mm, it can be easily clogged by suspended particles, chemical sediments, and microorganisms in the water, and the biofilm adhering to the inner wall of the pipe is the main reason for the clogging [9–12]. In addition, the presence of the biofilm brings a number of other problems, including the reduction of system performance (e.g., irrigation uniformity and system life) [10], health hazard [13], and food safety threats [14], which have become the main obstacles to the expanded application of RW in agriculture [15]. The existence of microorganisms is the most important prerequisite for biofilm formation. Therefore, to control biofilm formation in microirrigation systems, it is necessary to study in detail the development and growth potential of microorganisms in microbial biofilm communities and the characteristic changes in the microbial composition of biofilms under different conditions [16,17]. As a DNA sequencing technology, high-throughput sequencing is capable of sequencing hundreds of thousands to millions of DNA molecules simultaneously and provides highly sensitive and unbiased detection results to reveal the structure of the microbial community under study [18]. Currently, high-throughput sequencing techniques are used to elucidate the bacterial composition of young biofilms in drinking water distribution systems [19]. It was also used to demonstrate that biofilms exhibited different community structures when incubated on an unnatural substrate (microplastics) and two natural substrates (rocks and leaves) [20].

In this work, we compared the effects of three different types of RW on biofilm accumulation and system clogging in fresh DIS pipelines. We also analyzed the microbial composition in the different biofilms by high-throughput sequencing of 16S rRNA genes and identified the dominant and key microorganisms in the microbial community by analyzing the bacterial interactions. This study aims to better understand the accumulation process and characteristics of the biofilm microbial community in DIS, from the perspective of the microbial community and bacterial interaction, to provide clues for solving the problem of pipe clogging in agricultural use of reclaimed water utilization, improve the use efficiency of reclaimed water, and reduce the cost of system maintenance.

2. Materials and Methods

2.1. Agricultural Distribution System for Reclaimed Water

In an agricultural park in Tongzhou County, Beijing, the reclaimed water (RW) came from the secondary effluent of three sewage treatment plants, namely RW1 treated by a cyclic activated sludge system, RW2 treated by a rapid biochemical process, and RW3 treated by a sequential aeration system for wastewater reuse. During the experiment, the quality of the reclaimed water was analyzed and recorded using the online monitoring system of the sewage treatment plant (Table 1). The three sewage treatment processes are shown in Figure S1. The system consists of a water tank, valves, disc filters, pipes, dehumidifiers, valves, and reflux units, in which 120 mesh disc filters are cleaned every 3 days. In front of the horizontal inlet of the drip irrigation system (DIS) is a backflow unit consisting of two horizontal pipes and three vertical pipes. Valves are in front of the backflow unit and between the backflow unit and the horizontal inlet of the drip irrigation system. Therefore, the control of working pressure and flow is mainly by shunt principle, and the constant working pressure of 0.1 mpa is set every day before the experiment. To eliminate the temperature error, Honicom RJ 2–8.5 KW instantaneous water heater (Foshan, China) is connected to the system, and the water temperature of the system is stable at $25\text{ }^{\circ}\text{C} \pm 0.1\text{ }^{\circ}\text{C}$. The transverse length of the system is 6 m, and the distance between the emitters is 0.3 m. The non-pressure compensated flat emitter is manufactured by Netfilm, Israel, and the length \times width \times depth of the serrated flow channel is 35.79 mm \times 0.53 mm \times 0.75 mm, and the nominal flow rate is 1.6 L/h (Figure 1). The flow rate of the sprinkler in DIS is used to evaluate the system performance [17]. The flow meter at the head, middle, and end of each side of DIS was selected for a 3 min test, and the flow rate was weighted to determine

the degree of clogging of the system. The relative average flow (Dra) was calculated as previously described by Capra and Scicolone (2004).

Table 1. Diversity index of microbial community in biofilms.

Types of Reclaimed Water	Time	Diversity Index			
		ACE	Chao1	Shannon	1/Simpson
RW1	196 h	427	428	3.34	11.21
	294 h	468	475	4.02	29.79
	392 h	523	532	4.03	18.25
	490 h	813	834	4.45	46.01
	588 h	628	649	3.45	15.92
	784 h	619	523	4.16	14.18
RW2	196 h	735	742	4.09	22.75
	294 h	704	709	3.97	21.28
	392 h	736	698	4.35	34.57
	490 h	941	927	4.59	34.61
	588 h	863	861	4.40	23.07
	784 h	580	566	3.06	16.19
RW3	196 h	802	804	4.54	14.37
	294 h	761	748	4.22	27.34
	392 h	939	959	4.69	34.21
	490 h	964	989	5.13	58.49
	588 h	830	833	4.44	18.58
	784 h	786	794	4.57	13.73

2.2. Determination of Water Quality and Biofilm Composition

To determine the water quality of the reclaimed water, biochemical oxygen demand (BOD₅), total bacterial count (TB), total nitrogen (TN), and Cl⁻ were determined using the standard methods prescribed by the American Public Health Association APHA (2005) [21]. To collect biofilms, the selected emitter was cut from the side before the internal biofilms were collected. Specifically, the emitter samples were collected six times, e.g., after the system had been in operation for 196 h, 294 h, 392 h, 490 h, 588 h, and 784 h. The dry weight (DW) of biofilms was measured on a high-precision electronic balance (Hochoice, Shanghai, China) after ultrasonic cleaning (Shumei, Kunshan, China) [22]. Samples were weighed before and after membrane removal, and the dry weight value was subtracted from the two weighing values. Extracellular polysaccharide (EPR) and extracellular protein (EPO) were determined by phenol sulfuric acid colorimetry [23] and Lowry method [24], respectively.

2.3. High-Throughput Genomic Assay of Microorganisms in Biofilms

The suspension fluid of the biofilm was used to characterize the microbial community by bacterial 16S rRNA gene sequencing (Majorbio Scientific Ltd., Shanghai, China) on Roche Genome Sequencer FLX Sequencing Platform [25]. The 454 high-throughput sequencing method included extraction, amplification, purification, quantification, and homogenization. The obtained effective sequences in each library were further optimized and phylogenetically characterized using the QIIME software with the SILVA database. The operational taxonomic units (OTUs) of the biofilm were then generated using the Ribosomal Database Project (RDP, <http://rdp.cme.msu.edu> (accessed on 16 June 2020) Bayesian classifier at 70% threshold [26] and were identified to the level of phylum, class, order, family, and genus.

2.4. Ecological Network Analysis of Microbial Communities

A phylogenetic molecular ecological network was generated for the microbial communities based on the standardized relative abundances of the OTUs and their species classification. The microbial community diversity index was calculated according to the classification of OTUs, including community diversity (Shannon), dominance index (Simpson),

and community richness index (Chao1 and ACE) [27]. Differences in bacterial communities were revealed by weighted principal coordinate analysis (PCoA).

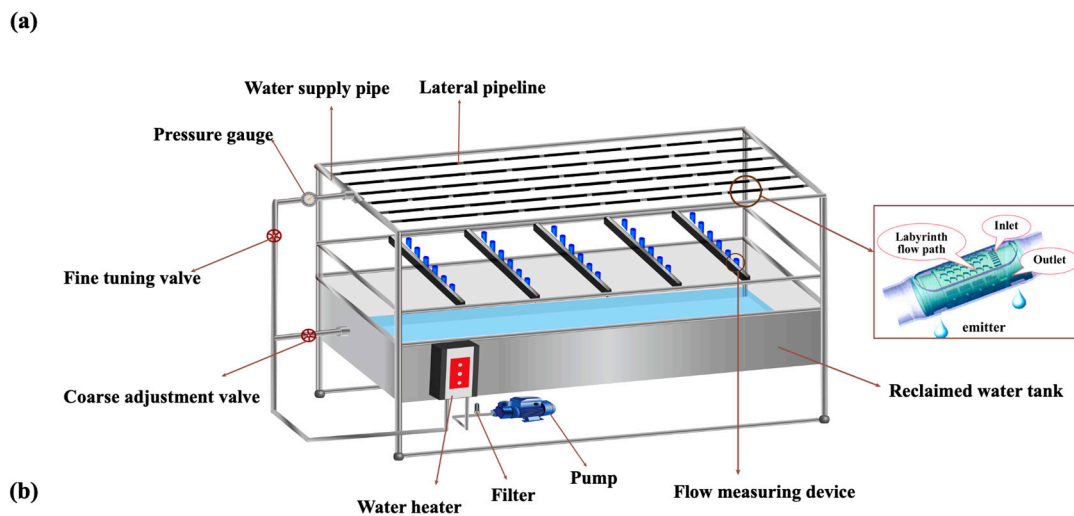


Figure 1. System setup in this work. (a) Layout of the agricultural reclaimed water distribution system for testing in this work; (b) A method diagram of the working principle in this work.

2.5. Statistical Analysis

The Wilcoxon rank-sum test was used to detect OTUs with significant differences in abundance between RW1/2/3 groups ($p < 0.05$). The BH method [28] was used to control the error detection rate. The R software (version 4.1.1) was used to analyze the significance of the diversity indicators between the different groups using the Wilcoxon rank-sum test. Differences between groups were analyzed by similarity analysis (ANOSIM) and molecular variance weighted analysis (AMOVA) using the Vegan package of R software (version 4.1.1). Spearman analysis [29] was used to analyze the correlation between water quality factors and biofilm composition. Cytoscape 3.9.0 software was used to create a vector plot showing the classification of OTU species and their correlation with the three water quality indicators.

3. Results and Discussion

3.1. System Performance and Biofilm Components in DIS Supplied by RW

In this study, the effects of three types of reclaimed water (RW1, RW2, and RW3) on biofilm formation and characteristics in a fresh drip irrigation system (DIS) were investigated over a period of 784 h. The reclaimed water used in this study was obtained from

three types of sewage after different treatments, and their quality indicators are shown in Table S1. The performance of DIS systems is evaluated by the relative average flow rate (Dra) [22]. Throughout the operation process, the extracellular protein (EPO) and extracellular polysaccharide (EPR) content of the RW3 biofilms were higher than those of the RW1 and RW2 biofilms, and the difference was particularly evident after 392 h (Figure 2b,c). The same trend was also reflected in the dry weight (DW) of the biofilms, i.e., the DW of the biofilms increased slowly from 0 to 392 h and rapidly after 392 h. After 490 h, the dry weight of biofilms produced under the three water conditions showed the largest difference (Figure 2a), which was consistent with the promoting effect of extracellular polymers on biofilm accumulation.

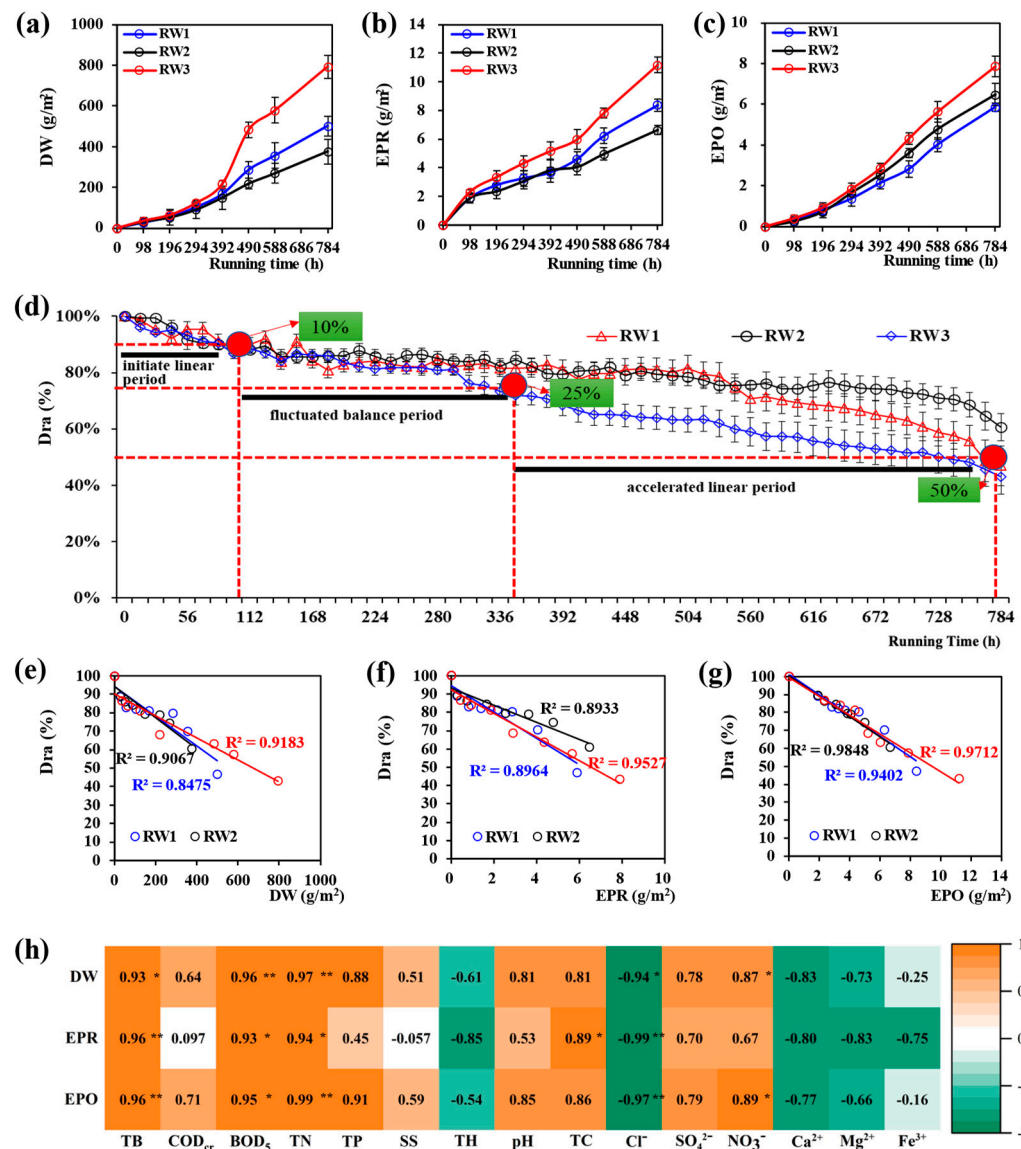


Figure 2. Biofilm composition and system performance of the drip irrigation system with RW1/2/3 as water sources. (a–c) The changes of DW, EPR, and EPO contents of biofilm, respectively; (d) The change pattern of Dra in the drip irrigation system under three reclaimed water conditions; (e–g) The correlation between Dra and DW, EPR, and EPO contents of biofilm, respectively; (h) The correlation between biofilm components and water quality. * indicates significance of $p < 0.05$, ** indicates significance of $p < 0.01$.

The accumulation of biofilms inevitably leads to clogging of DIS emitters [10]. In this study, the Dra of the DIS system initially showed a linear decline (0–196 h), then reached

equilibrium in fluctuation (196–490 h), and accelerated the linear decline in the later period (490–784 h) (Figure 2d). When the system ran at 784 h, DIS was the most clogged, and the clogging of the RW3 group was 43%, which was 8.3% and 28.9% less than the RW1 and RW2 groups, respectively (Figure 2d). Under the three water conditions, the correlation between biofilm components and clogging degree was 0.85–0.98, which was consistent with a previous report on another irrigation method, i.e., biofilm accumulation was the main factor leading to pipe clogging [30]. In this work, the correlation between EPR and clogging degree was the highest, and the correlation coefficient was >0.92 (Figure 2e–g).

Next, to determine which water quality indices of reclaimed water affect biofilm formation and thus cause clogging, we analyzed the correlation between 16 water quality indices and biofilm DW, EPR, and EPO. The results showed that BOD₅, total bacterial count (TB), and total nitrogen (TN) were positively correlated with biofilm formation, while Cl[−] concentration was negatively correlated (Figure 2h). BOD₅ represents the dissolved oxygen content used by microorganisms to degrade organic matter as a carbon source [31], while TB in reclaimed water provides essential nitrogen for microbial growth [32]. The concentration of Cl[−] in water can change the osmotic pressure of the cell surface, and when the concentration of Cl[−] is higher than 100 mg/L, the surface tension of the cell membrane changes and micropores are formed, leading to the leakage of K⁺ and other important ions, and cell death [33,34]. Therefore, the higher BOD₅, TB, and TN indices and lower Cl[−] concentration in RW3 compared with RW and RW2 could be the reason for the faster accumulation of biofilms under RW3 conditions.

3.2. Diversity and Dynamics of Microbial Biofilm Communities under Different Conditions of Reclaimed Water

In this section, 16S rRNA sequencing was used to analyze and classify the microbes in the biofilms formed under different water conditions, and to determine the major genera and their relative abundances in the microflora. A total of 22,480 effective V3–V4 variable regions of 16S rRNA were amplified with universal primers, and 337–823 operational taxonomic units (OTUs) were obtained with an identity level of 97%. The rarefaction curves were asymptotic, and the Good's coverage was higher than 0.99 (Figure S2), indicating that the sequencing reached sufficient depth [35]. The number of OTUs in the biofilms formed by the three RW types increased during the 196–490 h period and then decreased during 490–784 h. At 490 h, the number of OTUs reached the maximum and the number of OTUs in the RW3 biofilm was 22.1% and 13.4% higher than in the RW1 and RW2 biofilms, respectively (Figure 3a). In the later period (588–784 h), the number of OTUs fluctuated slightly, indicating that the microorganisms of the biofilm had adapted to the environment and had become stable (Figure 3a).

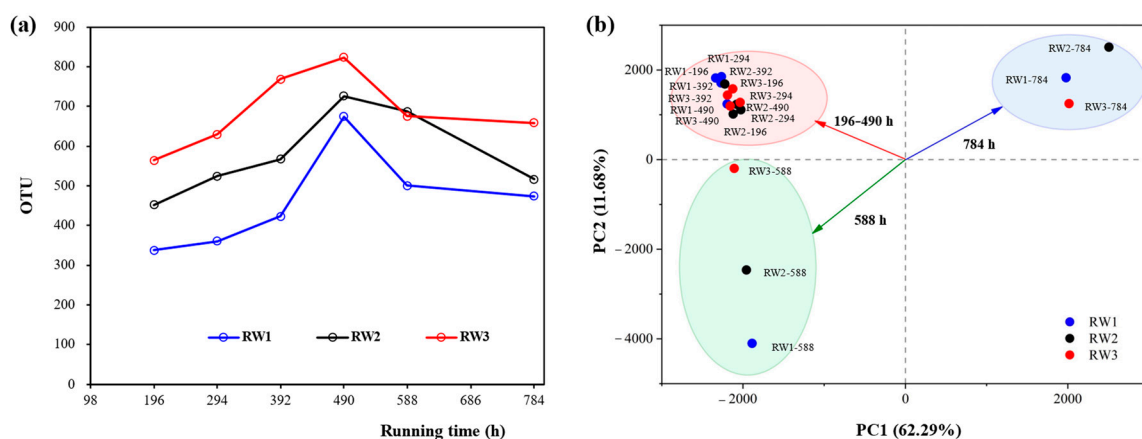


Figure 3. Variation patterns of OTUs in biofilms and principal component analysis of the microbial community. (a) Variation of OTUs in organisms; (b) Principal component analysis of microbial community in biofilm.

To further investigate the characteristics of the microbial communities in the biofilms formed under different water quality conditions, we analyzed the polymorphism parameters of the microbial communities in each biofilm. ACE and Chao1 were used to estimate community richness, and Shannon and Simpson reciprocals were used to estimate community diversity. ACE and Chao1 indices of the three biofilms increased steadily during 196–490 h and decreased rapidly during 490–784 h (Table 1). Both indices peaked at 490 h, indicating that community diversity was most complex at this time [36]. In addition, the community diversity of biofilms, as represented by the Shannon and Simpson reciprocals of the three types of biofilms, also reached the maximum at 490 h (Table 1), suggesting that this timepoint could be used as a critical point for controlling the growth of biofilms. When the β -diversity of the biofilm was analyzed using principal component analysis (PCoA), there was no significant difference among biofilms formed under the three water conditions, but there was a significant clustering of biofilms formed at different time periods (196–490 h, 490–588 h, and 588–784 h) (Figure 3b). On the first axis of the PCoA, the bacterial communities of the 196–490 h and 490–588 h groups were significantly different from those of the 588–784 h groups, and on the second axis, the bacterial communities of the 196–490 h and 490–588 h groups were clearly separated (Figure 3b).

3.3. Identification and Analysis of Microbial Community Composition and Key Microflora in Biofilms

The main bacteria in drinking water include *Proteobacteria*, *Actinobacteria*, *Firmicutes*, and *Bacteroidetes*. In this study, a total of 1191 OTUs belonging to 20 phyla were identified, with *Proteobacteria* and *Actinobacteria* dominating with a relative abundance of 13–15% and 11–13%, respectively. The 20 phyla were further classified into 47 classes, 97 orders, 149 families, 235 genera, and 318 species, of which 97.4% belonged to Bacteria and only 0.1% and 1.3% belonged to Archaea and Eukaryotes, respectively (Figure 4a). Moreover, the relative abundance of *Proteobacteria* in the biofilms showed an increasing trend from 10–15% to 17–22% during the 196–392 h phase. The relative abundance of *Actinobacteria*, *Chloroflexi*, and *Cyanobacteria* varied dynamically from 12% to 14%, 0.5% to 1.3%, and 0.1% to 1.1%, respectively, during the 196–392 h phase (Figure 4a). The most important changes after 392 h included that the relative abundance of *Proteobacteria* and *Actinobacteria* decreased by 69% and 63%, respectively, and the relative abundance of *Chloroflexi* and *Cyanobacteria* increased by 338% and 949%, respectively (Figure 4a). From 392 h to 490 h, the relative abundance of *Proteobacteria* in RW3 biofilms was 21% and 10% higher than in RW1 and RW2, respectively; and the relative abundance of *Actinobacteria* in the RW2 biofilms was 36% and 7% higher than in RW1 and RW3, respectively (Figure 4a).

Comparing the biofilms formed during the 196–392 h and 490–784 h periods, the number of OTUs with significant differences increased from 31 to 62. During 196–392 h, 31 differential OTUs were identified in RW1/2/3 biofilms (Figure 4b), with 5 OTUs distinguishing between RW1 and RW2 biofilms, including mainly *Caldilineaceae_bacterium* (OTU_140). In RW1 and RW3 biofilms, 19 significantly different OTUs mainly included *Parachlamydia_sp.* (OTU_1289), *Rhodobacter_ovatus* (OTU_408), and *Caldilineaceae_bacterium* (OTU_140). In RW2 and RW3 biofilms, 11 differential OTUs belonged mainly to *Flavobacterium_sp.* (OTU_1060), *Chryseobacterium_hispalense* (OTU_384), and *Gaetbulibacter_marinus* (OTU_443) (Figure 4b). Over the period 490–784 h, the number of OTUs with significant differences in biofilms formed under the three water conditions increased to 62 (Figure 4b as square nodes, triangular nodes, and V-shaped nodes), with 42 OTUs distinguishing RW1 from RW2 biofilms mainly including *Bacillus_luteus* (OTU_233), *Caldilineaceae_bacterium* (OTU_140), *Chryseobacterium_aquifrigidense* (OTU_1095), *Legionella_sp.* (OTU_1311), and *Protochlamydia_amoebophila* (OTU_888). In RW1 and RW3 biofilms, 29 differential OTUs were found, including *Caldilineaceae_bacterium* (OTU_140), *Cytophaga_hutchinsonii* (OTU_108), and *Jaaginema_geminatum* (OTU_215). For RW2 and RW3 biofilms, a total of 35 differential OTUs were identified, including mainly *Geobacillus_thermodenitrificans* (OTU_857), *Caldilineaceae_bacterium* (OTU_140), and *Nodosilinea_sp._IS-EAG2* (OTU_270) (Figure 4b).

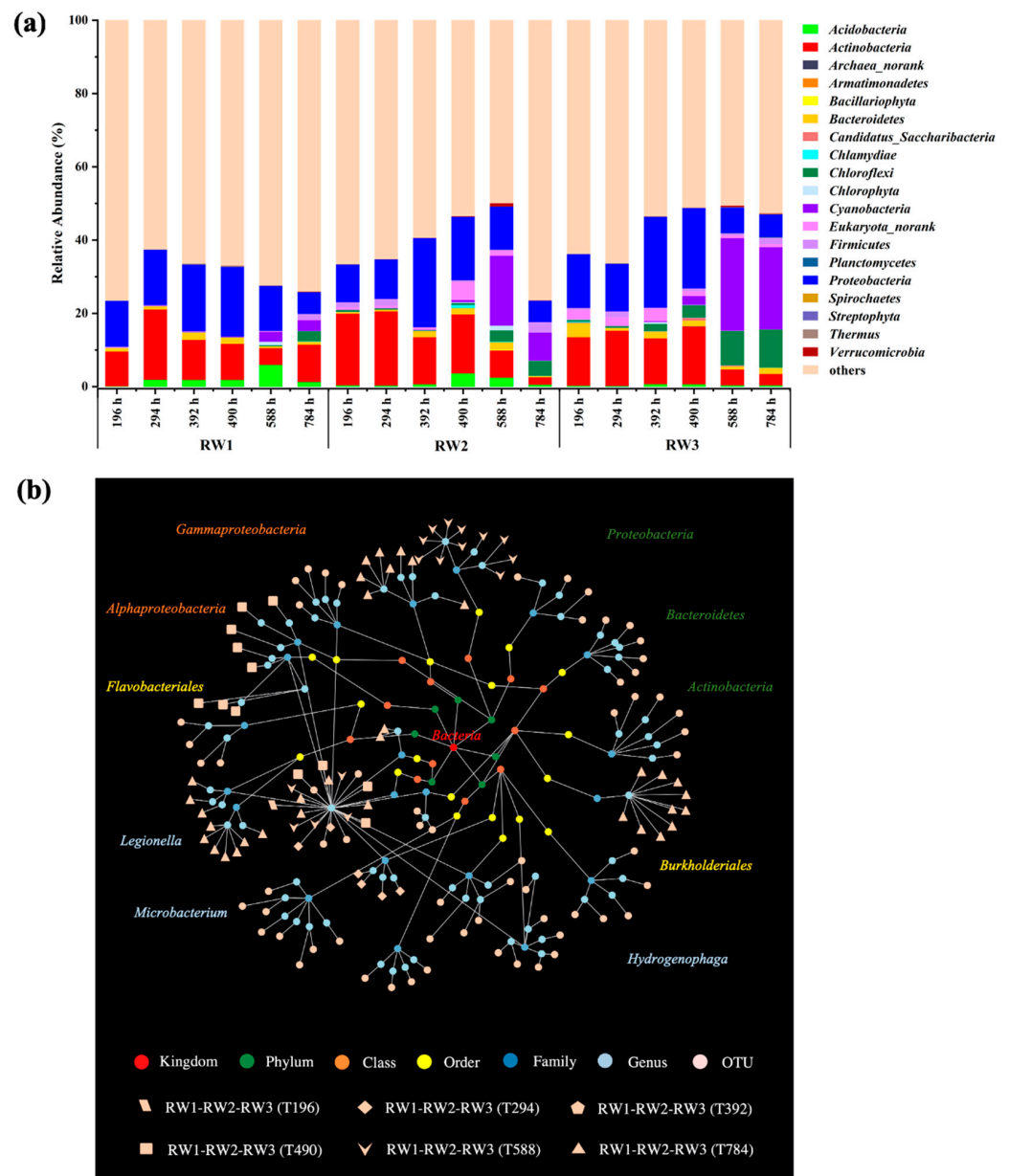


Figure 4. The taxonomic composition of bacteria and community structure in biofilms formed by three types of water sources. **(a)** The relative abundances of phyla in different samples; **(b)** Tree diagram of bacterial community classification in different samples. The nodes in the network diagram represent species at each classification level. The connection between the nodes represents the classification path of species from the root (bacteria) to the OTU level, and the OTU is the lowest classification node. Species at different levels were labeled with different colors, and the average relative abundance of species in the sample was indicated. Nodes with different shapes represent OTUs with significant differences ($p < 0.05$) in different comparisons. Multiple bacteria with significant differences are labeled with different colors depending on the level.

The above results show that the microbial flora in the three biofilms changed significantly, which were mainly *Bacillaceae*, *Legionellaceae*, *Leptolyngbyaceae*, and *Pseudanabaenaceae*. The RW1 biofilm and RW2 biofilm were dominated by *Legionellaceae* and *Leptolyngbyaceae*, respectively, while the RW3 biofilm was dominated by *Bacillaceae* and *Pseudanabaenaceae* (Figure 4b). In agreement with our results, biofilm bacterial communities have been shown to be dramatically affected by a variety of water quality parameters [37,38]. For example, *Legionellaceae* (which belong to the *Proteobacteria*) have been shown to be very sensitive to

environmental pH and nutrient availability [39]. *Bacillaceae* and *Pseudanabaenaceae* were sensitive to chlorine concentration in reclaimed water [37,38]. The concentration of Cl^- was the lowest in RW3 biofilms, while BOD_5 and total nitrogen (TN) were the highest, which could be the reason for the highest microbial population and microbial community richness in RW3 biofilms, and because these biofilms grow in large numbers on the wall of DIS, the pipes supplied with RW3 were more likely to be clogged than the pipes supplied with RW1 or RW2.

3.4. Microbial Interactions in Biofilm Formation under Different Reclaimed Water Conditions

In this section, we constructed phylogenetic molecular ecological networks (pMENs) to understand the patterns of bacterial co-occurrence and the basic topological properties of microbial interaction networks in the 196–392 h and 490–784 h periods. Compared with the 196–392 h phase, the positive interaction rate between OTUs increased significantly in the 490–784 h phase, indicating that 490 h is a critical timepoint (Figure S3 and Table S3). In the pMENs at 490 h under three water conditions, all network connectivity distributions conform to the power-law model ($R^2 > 0.80$) (Table 2), indicating that most bacteria are almost unrelated to other bacteria, whereas a few bacteria are related to several bacteria. After 490 h, the average connectivity (avgK) was higher in the RW3 group (8.42) than in the RW1 (6.33) and RW2 groups (7.91) (Table 2), indicating that the efficiency of information, energy, and mass transfer between the microbial species was higher in the RW3 biofilm. Because the transfer efficiency has a positive effect on the stability of the microbial community [4], its decrease can affect the structure of the microbial community and easily detach it. The empirical network size (the total number of nodes) of the RW1 group (80) and the RW3 group (82) was 9% and 7% smaller, respectively, than that of the RW2 group (88) (Table 2), indicating similar bacterial network complexity in the three biofilm types. The average geodesic distances (avgGD) in the three pMENs ranged from 2.7 to 4.2, indicating that the three networks had small-world properties with nodes closely connected to each other. Compared with the RW1 and RW2 networks, the avgGD of the RW3 network was much smaller (Table 2), suggesting a closer network interaction between the microbial constituents than in the RW1 and RW2 biofilms. In the biofilm, microorganisms with similar functions form modules, and the higher the degree of modularization, the more complex the organizational function of the biofilm and the stronger its resistance to environmental influences. The modularity in the three waters was 0.345 (RW1), 0.390 (RW2), and 0.530 (RW3), indicating that the RW3 biofilm has the most complex function and thus the most stable structure.

Table 2. Microbial community molecular ecological network topology parameters.

Treatment	Similarity Threshold (St)	Network Size (N)	R ² of Power Law	Average Connectivity (Avgk)	Average Clustering Coefficient (Avgcc)	Average Path Distance (GD)	Modularity	Module No.
RW1	0.980	80	0.375	6.325	0.304	4.194	0.345	4
RW2	0.980	88	0.377	7.909	0.192	2.780	0.390	10
RW3	0.980	82	0.333	8.415	0.208	2.709	0.530	5

Interactions between species include both symbiosis [40] and antagonism, both of which can influence biofilm formation and development [41]. In the overall pMENs, RW1, RW2, and RW3 groups had 346, 347, and 253 links, respectively, with the positive chains representing the symbiotic relationship between the microorganisms, their joint participation in biofilm formation, or the exchange of metabolites [42], while the negative chains represented the competitive or even predatory relationship [4]. The symbiotic interactions between bacteria (blue line) accounted for 53%, 32%, and 67% of the total links in RW1, RW2, and RW3 groups, respectively (Figure 5a–c). Compared to RW1 and RW2, the microorganisms in the RW3 biofilm have the strongest symbiotic relationship and the

weakest antagonistic effect, which increases the complexity of the microbial community structure and promotes the formation of the biofilm [41].

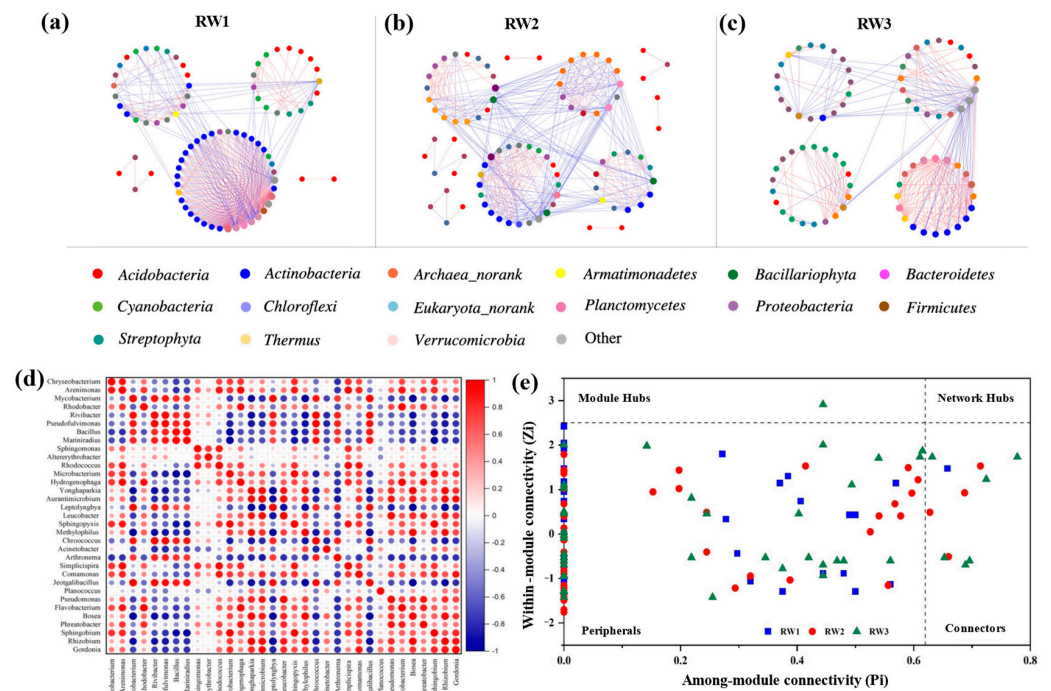


Figure 5. Interaction of bacterial networks in biofilms. (a–c) Visual co-occurrence networks of microbes in biofilms formed by RW1, RW2, and RW3, respectively. Red links indicate negative connections and blue links indicate positive connections between the OTUs; (d) Spearman correlation analysis among different bacterial genera (top 33). Each circle’s diameter and color are proportional to the correlation coefficients, and blue represents negative correlation while red represents positive correlation; (e) Zi-Pi plots based on the topological roles under different water sources.

To further clarify the interactions among the major microorganisms in biofilms, the interactions among the top 33 bacterial genera in biofilms were analyzed using the Spearman correlation method (Figure 5d). As the most abundant genus, *Microbacterium* (6.5%) showed significant positive correlations with *Sphingopyxis* (0.6%) and *Sphingobium* (0.2%), and significant negative correlations with *Bacillus* (0.2%) and *Mariniradius* (0.2%) (Figure 5d and Table S2). Meanwhile, there was a high positive correlation between two other dominant genera, *Sphingomonas* (2.1%) and *Rhodococcus* (1.2%) (Figure 5d and Table S2). As hydrophobic bacteria [43,44], the hydrophobicity of their surface could influence biofilm formation by regulating bacterial movement, adhesion, and growth [45–48]. In contrast, *Bacillus* (0.2%), *Mariniradius* (0.2%), and *Arthronema* (0.4%) showed negative correlations with most other genera, especially *Microbacterium* (6.5%) and *Hydrogenophaga* (2.0%), suggesting that they might play a key role in the bacterial community composition of biofilms through competitive relationships with other genera (Figure 5d). Indeed, some studies have shown that the artificial addition of antagonistic bacteria such as *Bacillus* to the microbial community could effectively control microbial growth [49–51].

When the topological roles of OTUs in three networks were plotted in a Z-P plot, nodes with $Z_i \geq 2.5$ or $P_i \geq 0.62$ were characterized as key species [52] and 91–99% of the OTU nodes were found to be peripheral ($Z_i < 2.5$ and $P_i < 0.62$) (Figure 5e). Only 1–6 OTU nodes were identified as connectors, i.e., species that produced a high degree of connectivity with several other modules ($P_i \geq 0.62$) (Figure 5e). The RW3 biofilm had six connectors, mainly *Flavobacterium_fontis* (OTU_582) and *Schlegelella_thermodepolymerans* (OTU_552), and one module hub (nodes that were highly connected to nodes within their modules), *Legionella_sp._LHG-1BW4* (OTU_582) (Figure 5e). The RW2 biofilm had four connectors,

including mainly *Roseococcus_sp._LW5* (OTU_421) and *Burkholderia* (OTU_1102), and the RW1 biofilm had only one critical OTU (connector), *Bacillus_sp.* (OTU_788) (Figure 5e). However, OTUs in the network hub region (overlap of module hub OTUs and connector OTUs) were not detected in any of the three water source biofilms (Figure 5e).

4. Conclusions

Clogging caused by biofilm hinders the application of reclaimed water in drip irrigation systems. Understanding the microbial composition of biofilm in drip irrigation systems and its dynamic change under different conditions can help to solve the problem of system clogging. In this study, BOD₅, total bacterial count (TB), and total nitrogen (TN) are the main factors that promote biofilm formation, while Cl⁻ concentration is the main factor that prevents biofilm formation, and their combined effect determines biofilm formation. Analysis of the microbial community structure in biofilm showed that 392–490 h is the key point for controlling the growth of biofilm. During 392–490 h, the relative abundance of *Proteobacteria* and *Actinobacteria* decreased significantly, while the relative abundance of *Chloroflexi* and *Cyanobacteria* increased significantly, resulting in dynamic changes in the bacterial community structure, network interaction, and network modularity of the biofilms. Microbial diversity peaked at 490 h, when community richness was greatest and symbiosis between bacterial strains was strongest, promoting biofilm formation. In addition, *Sphingomonas*, *Rhodococcus*, *Bacillus*, *Mariniradius* and *Arthronema* could be the key microbial species influencing the growth and proliferation of the other bacteria. Specific interventions targeting these key bacterial species could be effective in reducing overall bacterial populations and exploiting antagonistic interactions between bacteria to reduce biofilm accumulation. In summary, the research findings of this article provide technical support for further optimizing the performance of the DIS system, reducing system maintenance costs, and realizing safe and efficient irrigation of reclaimed water. In the future, we will continue to explore the technical methods and application models to reduce biofilm clogging in reclaimed water systems.

Supplementary Materials: The following supporting information can be downloaded at: <https://www.mdpi.com/article/10.3390/w14081216/s1>, Figure S1: Schematic diagram of three sewage treatment processes and reclaimed water agricultural micro-irrigation system; Figure S2: Rarefaction curve; Figure S3: Interaction of bacterial networks in biofilms. (a) Visible co-occurrence networks of microorganisms in biofilms formed during T196-T392 and T490-T784, respectively. Red links indicate negative connections and blue links indicate positive connections between the OTUs; (e) Zi-Pi plots based on the topologic roles under different time conditions; Table S1: Water quality indexes (mg/L); Table S2: The relative abundances and standard errors of bacteria in phylum, class, order, family and genus (%) (490 h); Table S3: Microbial community molecular ecological network topology parameters.

Author Contributions: Conceptualization, T.W.; formal analysis, T.W. and X.D.; investigation, T.Z., C.X. and Z.G.; project administration, J.W.; supervision, J.W.; visualization, X.D., T.Z., C.X. and Z.G.; writing—original draft, T.W. and X.D. All authors have read and agreed to the published version of the manuscript.

Funding: This research was funded by the National Natural Science Fund of China (No. 51321001 and 51808314) and the Independent Innovation Fund of Tianjin University (2021XZ-0019).

Institutional Review Board Statement: Not applicable.

Informed Consent Statement: Not applicable.

Data Availability Statement: The datasets generated during and/or analyzed during the current study are available from the corresponding author upon reasonable request.

Conflicts of Interest: The authors declare that they have no known competing financial interest or personal relationship that could have appeared to influence the work reported in this paper.

References

1. Amarasinghe, U.A.; Smakhtin, V. *Global Water Demand Projections: Past, Present and Future*; International Water Management Institute (IWMI): Colombo, Sri Lanka, 2014.
2. Bijl, D.L.; Bogaart, P.W.; Kram, T.; de Vries, B.J.M.; van Vuuren, D.P. Long-term water demand for electricity, industry and households. *Environ. Sci. Policy* **2016**, *55*, 75–86. [[CrossRef](#)]
3. Cherchi, C.; Kesaano, M.; Badruzzaman, M.; Schwab, K.; Jacangelo, J.G. Municipal reclaimed water for multi-purpose applications in the power sector: A review. *J. Environ. Manag.* **2019**, *236*, 561–570. [[CrossRef](#)] [[PubMed](#)]
4. Deng, S.; Yan, X.; Zhu, Q.; Liao, C. The utilization of reclaimed water: Possible risks arising from waterborne contaminants. *Environ. Pollut.* **2019**, *254*, 113020. [[CrossRef](#)] [[PubMed](#)]
5. Li, Q.; Wang, W.; Jiang, X.; Lu, D.; Zhang, Y.; Li, J. Analysis of the potential of reclaimed water utilization in typical inland cities in northwest China via system dynamics. *J. Environ. Manag.* **2020**, *270*, 110878. [[CrossRef](#)] [[PubMed](#)]
6. Meneses, M.; Pasqualino, J.C.; Castells, F. Environmental assessment of urban wastewater reuse: Treatment alternatives and applications. *Chemosphere* **2010**, *81*, 266–272. [[CrossRef](#)] [[PubMed](#)]
7. Angelakis, A.N.; Bontoux, L. Wastewater reclamation and reuse in Eureau countries. *Water Policy* **2001**, *3*, 47–59. [[CrossRef](#)]
8. Dery, J.L.; Rock, C.M.; Goldstein, R.R.; Onumajuru, C.; Brassill, N.; Zozaya, S.; Suri, M.R. Understanding grower perceptions and attitudes on the use of nontraditional water sources, including reclaimed or recycled water, in the semi-arid Southwest United States. *Environ. Res.* **2019**, *170*, 500–509. [[CrossRef](#)]
9. Hills, D.J.; Brenes, M.J. Microirrigation of wastewater effluent using drip tape. *Appl. Eng. Agric.* **2001**, *17*, 303–308. [[CrossRef](#)]
10. Hou, P.; Wang, T.; Zhou, B.; Song, P.; Zeng, W.; Muhammad, T.; Li, Y. Variations in the microbial community of biofilms under different near-wall hydraulic shear stresses in agricultural irrigation systems. *Biofouling* **2020**, *36*, 44–55. [[CrossRef](#)]
11. Li, Y.K.; Liu, Y.Z.; Li, G.B.; Xu, T.W.; Liu, H.S.; Ren, S.M.; Yan, D.Z.; Yang, P.L. Surface topographic characteristics of suspended particulates in reclaimed wastewater and effects on clogging in labyrinth drip irrigation emitters. *Irrig. Sci.* **2012**, *30*, 43–56. [[CrossRef](#)]
12. Yan, D.; Bai, Z.; Rowan, M.; Gu, L.; Ren, S.; Yang, P. Biofilm structure and its influence on clogging in drip irrigation emitters distributing reclaimed wastewater. *J. Environ. Sci.* **2009**, *21*, 834–841. [[CrossRef](#)]
13. Blaustein, R.A.; Shelton, D.R.; Van Kessel, J.A.S.; Karns, J.S.; Stocker, M.D.; Pachepsky, Y.A. Irrigation waters and pipe-based biofilms as sources for antibiotic-resistant bacteria. *Environ. Monit. Assess.* **2016**, *188*, 56. [[CrossRef](#)] [[PubMed](#)]
14. Ngan, W.Y.; Habimana, O. From farm-scale to lab-scale: The characterization of engineered irrigation water distribution system biofilm models using an artificial freshwater source. *Sci. Total Environ.* **2020**, *698*, 134025. [[CrossRef](#)] [[PubMed](#)]
15. Duran-Ros, M.; Puig-Bargues, J.; Arbat, G.; Barragan, J.; de Cartagena, F.R. Effect of filter, emitter and location on clogging when using effluents. *Agric. Water Manag.* **2009**, *96*, 67–79. [[CrossRef](#)]
16. Escudie, R.; Cresson, R.; Delgenes, J.-P.; Bernet, N. Control of start-up and operation of anaerobic biofilm reactors: An overview of 15 years of research. *Water Res.* **2011**, *45*, 1–10. [[CrossRef](#)]
17. Zhou, B.; Wang, T.; Li, Y.; Bralts, V. Effects of microbial community variation on bio-clogging in drip irrigation emitters using reclaimed water. *Agric. Water Manag.* **2017**, *194*, 139–149. [[CrossRef](#)]
18. Franzosa, E.A.; Hsu, T.; Sirota-Madi, A.; Shafquat, A.; Abu-Ali, G.; Morgan, X.C.; Huttenhower, C. Sequencing and beyond: Integrating molecular ‘omics’ for microbial community profiling. *Nat. Rev. Microbiol.* **2015**, *13*, 360–372. [[CrossRef](#)]
19. Li, W.; Tan, Q.; Zhou, W.; Chen, J.; Li, Y.; Wang, F.; Zhang, J. Impact of substrate material and chlorine/chloramine on the composition and function of a young biofilm microbial community as revealed by high-throughput 16S rRNA sequencing. *Chemosphere* **2020**, *242*, 125310. [[CrossRef](#)]
20. Wu, X.; Pan, J.; Li, M.; Li, Y.; Bartlam, M.; Wang, Y. Selective enrichment of bacterial pathogens by microplastic biofilm. *Water Res.* **2019**, *165*, 114979. [[CrossRef](#)]
21. APHA. *Standard Methods for the Examination of Water and Wastewater*, 21st ed.; American Public Health Association: Washington, DC, USA, 2005.
22. Wang, T.; Guo, Z.; Shen, Y.; Cui, Z.; Goodwin, A. Accumulation mechanism of biofilm under different water shear forces along the networked pipelines in a drip irrigation system. *Sci. Rep.* **2020**, *10*, 6960. [[CrossRef](#)]
23. Nocker, A.; Lepo, J.E.; Martin, L.L.; Snyder, R.A. Response of estuarine biofilm microbial community development to changes in dissolved oxygen and nutrient concentrations. *Microb. Ecol.* **2007**, *54*, 532–542. [[CrossRef](#)] [[PubMed](#)]
24. Lowry, O.H.; Rosebrough, N.J.; Farr, A.L.; Randall, R.J. Protein measurement with the Folin phenol reagent. *J. Biol. Chem.* **1951**, *193*, 265–275. [[CrossRef](#)]
25. Herlemann, D.P.R.; Lundin, D.; Labrenz, M.; Juergens, K.; Zheng, Z.; Aspeborg, H.; Andersson, A.F. Metagenomic De Novo Assembly of an Aquatic Representative of the Verrucomicrobial Class Spartobacteria. *mBio* **2013**, *4*, e00569-12. [[CrossRef](#)] [[PubMed](#)]
26. Edgar, R.C. UPARSE: Highly accurate OTU sequences from microbial amplicon reads. *Nat. Methods* **2013**, *10*, 996–998. [[CrossRef](#)]
27. Schloss, P.D.; Westcott, S.L.; Ryabin, T.; Hall, J.R.; Hartmann, M.; Hollister, E.B.; Lesniewski, R.A.; Oakley, B.B.; Parks, D.H.; Robinson, C.J.; et al. Introducing mothur: Open-Source, Platform-Independent, Community-Supported Software for Describing and Comparing Microbial Communities. *Appl. Environ. Microbiol.* **2009**, *75*, 7537–7541. [[CrossRef](#)]
28. Benjamini, Y.; Hochberg, Y. Controlling the False Discovery Rate: A Practical and Powerful Approach to Multiple Testing. *J. R. Stat. Soc. Ser. B* **1995**, *57*, 289–300. [[CrossRef](#)]

29. Artusi, R.; Verderio, P.; Marubini, E. Bravais-Pearson and Spearman correlation coefficients: Meaning, test of hypothesis and confidence interval. *Int. J. Biol. Markers* **2002**, *17*, 148–151. [[CrossRef](#)]
30. Zhou, B.; Li, Y.; Liu, Y.; Xu, F.; Pei, Y.; Wang, Z. Effect of drip irrigation frequency on emitter clogging using reclaimed water. *Irrig. Sci.* **2015**, *33*, 221–234. [[CrossRef](#)]
31. Tang, D.; Zhai, X.; Zhang, G. Effects of Microorganisms Impacting on the Determination of Biochemical Oxygen Demand. *Environ. Prot. Oil Gas Fields* **2017**, *27*, 38–61.
32. Huang, S.; Voutchkov, N.; Jiang, S. Balancing carbon, nitrogen and phosphorus concentration in seawater as a strategy to prevent accelerated membrane biofouling. *Water Res.* **2019**, *165*, 114978. [[CrossRef](#)]
33. Chung, C.M.; Tobino, T.; Cho, K.; Yamamoto, K. Alleviation of membrane fouling in a submerged membrane bioreactor with electrochemical oxidation mediated by in-situ free chlorine generation. *Water Res.* **2016**, *96*, 52–61. [[CrossRef](#)] [[PubMed](#)]
34. Fan, B.; Carvalhais, L.C.; Becker, A.; Fedoseyenko, D.; von Wiren, N.; Borriss, R. Transcriptomic profiling of *Bacillus amyloliquefaciens* FZB42 in response to maize root exudates. *BMC Microbiol.* **2012**, *12*, 116. [[CrossRef](#)] [[PubMed](#)]
35. Gonzalez-Silva, B.M.; Jonassen, K.R.; Bakke, I.; Ostgaard, K.; Vadstein, O. Nitrification at different salinities: Biofilm community composition and physiological plasticity. *Water Res.* **2016**, *95*, 48–58. [[CrossRef](#)] [[PubMed](#)]
36. Inaba, T.; Aoyagi, T.; Hori, T.; Charfi, A.; Suh, C.; Lee, J.H.; Sato, Y.; Ogata, A.; Aizawa, H.; Habe, H. Clarifying prokaryotic and eukaryotic biofilm microbiomes in anaerobic membrane bioreactor by non-destructive microscopy and high-throughput sequencing. *Chemosphere* **2020**, *254*, 126810. [[CrossRef](#)]
37. Belila, A.; El-Chakhtoura, J.; Otaibi, N.; Muyzer, G.; Gonzalez-Gil, G.; Saikaly, P.E.; Loosdrecht, M.C.M.v.; Vrouwenvelder, J.S. Bacterial community structure and variation in a full-scale seawater desalination plant for drinking water production. *Water Res.* **2016**, *94*, 62–72. [[CrossRef](#)]
38. Xiao, Y.; Seo, Y.; Lin, Y.; Li, L.; Muhammad, T.; Ma, C.; Li, Y. Electromagnetic fields for biofouling mitigation in reclaimed water distribution systems. *Water Res.* **2020**, *173*, 115562. [[CrossRef](#)]
39. Newton, R.J.; Jones, S.E.; Eiler, A.; McMahon, K.D.; Bertilsson, S.A. A Guide to the Natural History of Freshwater Lake Bacteria. *Microbiol. Mol. Biol. Rev.* **2011**, *75*, 14–49. [[CrossRef](#)]
40. Liu, W.; Roder, H.L.; Madsen, J.S.; Bjarnsholt, T.; Sorensen, S.J.; Burmolle, M. Interspecific Bacterial Interactions are Reflected in Multispecies Biofilm Spatial Organization. *Front. Microbiol.* **2016**, *7*, 1366. [[CrossRef](#)]
41. Simoes, L.C.; Simoes, M.; Vieira, M.J. Influence of the Diversity of Bacterial Isolates from Drinking Water on Resistance of Biofilms to Disinfection. *Appl. Environ. Microbiol.* **2010**, *76*, 6673–6679. [[CrossRef](#)]
42. Layeghifard, M.; Hwang, D.M.; Guttman, D.S. Disentangling Interactions in the Microbiome: A Network Perspective. *Trends Microbiol.* **2017**, *25*, 217–228. [[CrossRef](#)]
43. Gargiulo, G.; Bradford, S.A.; Simunek, J.; Ustohal, P.; Vereecken, H.; Klumpp, E. Bacteria transport and deposition under unsaturated flow conditions: The role of water content and bacteria surface hydrophobicity. *Vadose Zone J.* **2008**, *7*, 406–419. [[CrossRef](#)]
44. Kawahara, K.; Mizuta, I.; Katabami, W.; Koizumi, M.; Wakayama, S. Isolation of *Sphingomonas* Strains from Ears of Rice and Other Plants of Family Gramineae. *Biosci. Biotechnol. Biochem.* **2014**, *58*, 600–601. [[CrossRef](#)]
45. Choi, N.-Y.; Bae, Y.-M.; Lee, S.-Y. Cell surface properties and biofilm formation of pathogenic bacteria. *Food Sci. Biotechnol.* **2015**, *24*, 2257–2264. [[CrossRef](#)]
46. Gallardo-Moreno, A.M.; Gonzalez-Martin, M.L.; Perez-Giraldo, C.; Bruque, J.M.; Gomez-Garcia, A.C. Serum as a factor influencing adhesion of *Enterococcus faecalis* to glass and silicone. *Appl. Environ. Microbiol.* **2002**, *68*, 5784–5787. [[CrossRef](#)]
47. Wu, L.; Dong, P.; Zhang, Y.; Mao, Y.; Liang, R.; Yang, X.; Zhu, L.; Luo, X. Biofilm Formation Ability of *Escherichia coli* O157:H7 on Stainless Steel Surface and Its Relationship with Bacterial Characteristics. *Food Sci.* **2020**, *41*, 127–132.
48. Zhang, M.-l.; Xu, S.-f.; Xu, M.-y.; Wang, L.; Chai, S.-s.; Bai, M.; Zhang, C. Study on microbial surface hydrophobicity under multiphase interface of water distribution network. *China Environ. Sci.* **2019**, *39*, 4823–4830.
49. Calvo-Garrido, C.; Roudet, J.; Aveline, N.; Davidou, L.; Dupin, S.; Fermaud, M. Microbial Antagonism Toward Botrytis Bunch Rot of Grapes in Multiple Field Tests Using One *Bacillus ginsengihumi* Strain and Formulated Biological Control Products. *Front. Plant Sci.* **2019**, *10*, 105. [[CrossRef](#)]
50. Schonbichler, A.; Diaz-Moreno, S.M.; Srivastava, V.; McKee, L.S. Exploring the Potential for Fungal Antagonism and Cell Wall Attack by *Bacillus subtilis* natto. *Front. Microbiol.* **2020**, *11*, 521. [[CrossRef](#)]
51. Soufi, R.E.; Bouzdoudi, B.E.; Bouras, M.; Kbiach, M.L.B.E.; Badoc, A.; Lamarti, A. Assessment of the Effect of Environmental Factors on the Antagonism of *Bacillus amyloliquefaciens* and *Trichoderma harzianum* to *Colletotrichum acutatum*. *Adv. Microbiol.* **2017**, *7*, 729–742. [[CrossRef](#)]
52. Feng, K.; Zhang, Z.; Cai, W.; Liu, W.; Xu, M.; Yin, H.; Wang, A.; He, Z.; Deng, Y. Biodiversity and species competition regulate the resilience of microbial biofilm community. *Mol. Ecol.* **2017**, *26*, 6170–6182. [[CrossRef](#)]